# Source-independent full waveform inversion of seismic data

Ki Ha Lee [*] and Hee Joon Kim[**]

## ABSTRACT

A rigorous full waveform inversion of seismic data has been a challenging subject partly because of the lack of precise knowledge of the source. Since currently available approaches involve some form of approximations to the source, inversion results are subject to the quality and the choice of the source information used. We propose a new full waveform inversion methodology that does not involve source spectrum information. Thus potential inversion errors due to source estimation can be eliminated. A gather of seismic traces is first Fourier-transformed into the frequency domain and a normalized wavefield is obtained for each trace in the frequency domain. Normalization is done with respect to the frequency response of a reference trace selected from the gather, so the complex-valued normalized wavefield is dimensionless. The source spectrum is eliminated during the normalization procedure. With its source spectrum eliminated, the normalized wavefield allows us construction of an inversion algorithm without the source information. The inversion algorithm minimizes misfits between measured normalized wavefield and numerically computed normalized wavefield. The proposed approach has been successfully demonstrated using a simple two-dimensional scalar problem.

## INTRODUCTION

It is a common practice in seismic industry to estimate subsurface velocity structure by analyzing the traveltimes of the seismic signals. In crosshole and surface-to-borehole applications, typical approaches involve ray tomography (e.g., Peterson et al., 1985; Nolet, 1985, Humphreys and Clayton, 1988; Scales et al., 1988; Vasco, 1991) and more recently Fresnel volume tomography (e.g., Cerveny and Soares, 1992; Vasco et al., 1995). Traveltime tomographies using ray tracing require high-frequency approximation, with maximum resolution on the order of a wavelength (Sheng and Schuster, 2000), or a fraction (5 %) of the well separation in some practical cases. Due to lack of resolution, however, usefulness of ray tomography may be limited if the objective is to better understand the petrophysical and hydrological properties of soils and rocks. Such understanding is important in characterizing petroleum and geothermal reservoirs and in environmental applications of various scales.

An alternative to traveltime tomography is full waveform inversion. Recent studies (e.g., Sen and Stoffa, 1991; Kormendi and Dietrich, 1991; Minkoff and Symes, 1997; Zhou et al., 1997; Plessix and Bork, 1998; Pratt, 1999a, 1999b) suggest that full waveform inversion can provide improved resolution of the velocity and density structures. Amplitudes and phases of waveforms are sensitive to the petrophysical property of the materials through which the wave propagates. Therefore, full waveform analyses may be used as tools in

[*] Ernest Orlando Lawrence Berkeley National Laboratory, MS 90-1116, Berkeley, California 94720. E-mail: KHLee@lbl.gov

[**] Pukyung National University, 599-1 Daeyoun-dong, Nam-gu, Busan 608-737, Korea. E-mail: hejkim@pknu.ac.kr.

investigating hydrological and petrophysical properties of the medium. There is, however, one major difficulty to overcome in full waveform inversion. In all field applications, the effective source waveform, the coupling between the source and the medium, and the coupling between the receivers and the medium, are not very well understood. The problem can be alleviated to some extent with a good velocity approximation (Pratt, 1999a), but the measured signals cannot be properly calibrated in general, rendering full waveform inversion technically difficult to apply.

In this paper we propose a methodology to overcome the above difficulty. The approach first transforms seismic data into the frequency domain and a set of normalized wavefield is constructed. The normalized wavefield is independent of the spectrum of the source, so the proposed method allows full waveform inversion without requiring the knowledge of the source signature. Frazer et al. (1997) and Frazer and Sun (1998) presented an inversion scheme for interpreting well-log sonic waveform data. In principle their approach is also source-independent, but it requires a source function as a necessary part of the inversion procedure. As a result the performance of inversion may depend on the source function chosen.

## NORMALIZED WAVEFIELD

Let us assume a seismic field survey involving *NS* source positions and *NG* receiver positions. The source-receiver configuration depends on the survey objective and the placement of sources and receivers is directed to ensure proper subsurface illumination. The proposed full waveform inversion scheme can be applied to analyzing data obtained from arbitrary configurations; surface or single borehole reflection, surface-to-borehole or borehole-to surface (VSP), or crosshole.

To demonstrate the validity of the proposed inversion scheme we consider a simple acoustic problem. The field data, in general, may be described as

$$D^d_{ji}(t) = R_j(t) * P^d_{ji}(t) * S_i(t),\ j = 1, 2, \ldots, NG,\ \ i = 1, 2, \ldots, NS, \qquad (1)$$

where * denotes convolution in time, and the superscript *d* indicates data from the true medium. We retain the superscript *d* here because we will be referring to the computer-generated model data using the superscript *m* later in this paper. Here $D^d_{ji}(t)$ is the pressure measurement at the *j*-th receiver position due to a source $S_i(t)$ at the *i*-th source position. The source function includes the source-medium coupling, and therefore is an effective source. $P^d_{ji}(t)$ is the impulse response of the true medium at the *j*-th receiver position due to a source at the *i*-th source position. The receiver function $R_j(t)$ includes the medium-receiver coupling as well. In the following analysis we will drop $R_j(t)$ by assuming that receiver (geophone) calibration is known and that the effect of medium-receiver coupling to data can be ignored in comparison with that corresponding to the source.

If we Fourier-transform equation (1), $FT\{(D, P, S)(t)\} \rightarrow (d, p, s)(\omega)$, ignoring $R_j(t)$ factor, we get

$$d_{ji}^{d}(\omega) = p_{ji}^{d}(\omega) s_i(\omega), \tag{2}$$

where $\omega$ is the angular frequency equal to $2\pi$ times the temporal frequency $f$. Convolution in the time domain is now direct multiplication in the frequency domain.

Next, to define the normalized wavefield, we first select the reference receiver, say with $j = 1$. The normalized wavefield $t_{ji}^{d}$ is defined in such a way that $t_{ji}^{d} = d_{ji}^{d} / d_{1i}^{d}$, $j = 2,\ldots,$ $NG$. It has a property of generating data at the $j$-th receiver position when it is multiplied by the data at the reference point. Rewriting, and using the relation given by equation (2), we get

$$t_{ji}^{d}(\omega) = \frac{d_{ji}^{d}(\omega)}{d_{1i}^{d}(\omega)} = \frac{p_{ji}^{d}(\omega) s_i(\omega)}{p_{1i}^{d}(\omega) s_i(\omega)} = \frac{p_{ji}^{d}(\omega)}{p_{1i}^{d}(\omega)}. \tag{3}$$

Here, the source spectrum cancels out itself, so the normalized wavefield is the same as the normalized impulse response of the medium.

## FULL WAVEFORM INVERSION

In this section we show that the normalized wavefield, or the normalized impulse response defined by equation (3), is adequate as input for the full waveform inversion. In other words, information in misfits in normalized wavefields is sufficient in constructing the objective functional for the inversion. We generate synthetic data for a given set of model parameters using an appropriate numerical method. From the synthetic data, normalized wavefield will be obtained for the given model, and it will be compared with the data given by equation (3) to get the misfit.

The proposed inversion scheme using the normalized wavefield is tested using a simple two-dimensional (2-D) acoustic model. Let us consider the impulse response governed by a 2-D acoustic wave equation in the frequency domain,

$$\nabla^2 p(\mathbf{x}, \mathbf{x}_s, \omega) + \frac{\omega^2}{v^2(\mathbf{x})} p(\mathbf{x}, \mathbf{x}_s, \omega) + \delta(\mathbf{x} - \mathbf{x}_s) = 0, \tag{4}$$

where the impulse response $p$ is the scalar pressure wavefield, $v$ is the velocity, and ($\mathbf{x}$, $\mathbf{x}_s$) are the field and source positions in 2-D. The source is an impulse point source expressed as a 2-D spatial delta function $\delta(\mathbf{x}\text{-}\mathbf{x}_s)$ located at $\mathbf{x}_s$. The source is also a delta function $\delta(t)$ at $t = 0$ in the time-domain. To obtain the numerical solution of equation (4), the spatial domain is first divided into a number of square elements of equal size, and a finite-element modeling (Marfurt, 1984; Pratt, 1990) scheme is used. Details of the finite-element method (FEM) may be found in many textbooks (e.g., Zienkiewicz and Taylor, 1989). The model parameter is the acoustic velocity in each of the square elements. After a numerical solution for the impulse response is obtained, the synthetic normalized wavefield is obtained for the impulse response of the given velocity model

$$t_{ji}^{m}(\omega) = \frac{p_{ji}^{m}(\omega)}{p_{1i}^{m}(\omega)}, \qquad j = 1, 2, \ldots, NG, \; i = 1, 2, \ldots, NS, \tag{5}$$

where superscript *m* is used to denote the impulse response for the prescribed model to distinguish it from the recorded responses superscripted by *d* for the true model (see equation (3)).

The inversion procedure minimizes the difference between normalized wavefields given by equations (3) and (5). The misfit functional to be minimized may be formally written as

$$\phi(\mathbf{m}) = \left\| \mathbf{W}_d (\mathbf{T}^m - \mathbf{T}^d) \right\|^2, \tag{6}$$

where $\|\bullet\|^2$ denotes the L2 norm and $\mathbf{W}_d$ is used to account for the measurement errors in the data. For data with uncorrelated errors $\mathbf{W}_d$ is a diagonal matrix whose elements are the inverse of the standard deviation of measurement errors. The column vector $(\mathbf{T}^m - \mathbf{T}^d)$ consists of misfits in normalized wavefield, and the parameter vector **m** represents the acoustic velocity in the square elements. The misfit at the reference data position is always zero $\left(t_{1i}^m = t_{1i}^d\right)$. The misfit vector $(\mathbf{T}^m - \mathbf{T}^d)$ has both real and imaginary parts, so the actual number of data points used for the inversion is $NEQ = 2 \times NFREQ \times NS \times (NG\text{-}1)$. Here, the variable *NFREQ* is the number of frequencies used for the inversion. $\mathbf{W}_d$ is an $NEQ \times NEQ$ square matrix, and the data misfit $(\mathbf{T}^m - \mathbf{T}^d)$ is an $NEQ \times 1$ column matrix.

We use the Gauss-Newton method for the inversion by first expanding the objective functional, equation (6), into a Taylor series (e.g., Bertsekas, 1982; Tarantola, 1987; Oldenburg et al., 1993)

$$\phi(\mathbf{m} + \delta\mathbf{m}) = \phi(\mathbf{m}) + \boldsymbol{\gamma}_m^T \delta\mathbf{m} + 0.5\delta\mathbf{m}^T \mathbf{H}_m \delta\mathbf{m} + O\{(\delta\mathbf{m})^3\}. \tag{7}$$

Here, $\delta\mathbf{m}$ is a perturbation to the model parameter $\mathbf{m}$, $\boldsymbol{\gamma}_m$ is an $M \times 1$ column matrix consisting of elements

$$\frac{\partial\phi}{\partial m_q}, \; q = 1, 2, \ldots, M,$$

with *M* being the total number of parameters to be determined. Explicitly, it is written as

$$\boldsymbol{\gamma}_m = 2\mathbf{J}^T \mathbf{W}_d{}^T \mathbf{W}_d \left(\mathbf{T}^m - \mathbf{T}^d\right),$$

where **J** is the Jacobian (sensitivity) matrix (see equation (8) mbelow). $\mathbf{H}_m$ is an $M \times M$ square (Hessian) matrix consisting of elements

$$\frac{\partial^2\phi}{\partial m_q \partial m_r}, \qquad q, r = 1, 2, \ldots, M,$$

compactly written as

$$\mathbf{H}_m = 2\mathbf{J}^T \mathbf{W}_d{}^T \mathbf{W}_d \mathbf{J} + O\left(\frac{\partial \boldsymbol{J}}{\partial \mathbf{m}}\right).$$

The last term of this equation represents the changes in the partial derivatives of data (normalized wavefield in this case) due to changes in the parameter **m**. This term is small if either the residuals are small, or the forward differential equation is quasi-linear (Tarantola, 1987). The term is usually difficult to compute and is generally ignored. For each frequency and source the sensitivity function **J** is a $\left[2\times(NG-1)\right]\times M$ rectangular matrix. For example, for the *i*-th source at a fixed frequency, the entries to the Jacobian corresponding to the *j*-th receiver and the *q*-th model parameter may be evaluated as

$$\begin{pmatrix} J_{q,(2*j-1),i} \\ J_{q,(2*j),i} \end{pmatrix} = \begin{pmatrix} \text{real part of}\left(\dfrac{\partial T_{ji}^m}{\partial m_q}\right) \\ \text{imaginary part of}\left(\dfrac{\partial T_{ji}^m}{\partial m_q}\right) \end{pmatrix}, \tag{8}$$

with

$$\frac{\partial t_{ji}^m}{\partial m_q} = \frac{\partial}{\partial m_q}\frac{p_{ji}^m}{p_{1i}^m} = \frac{1}{p_{1i}^m}\left(\frac{\partial p_{ji}^m}{\partial m_q} - \frac{p_{ji}^m}{p_{1i}^m}\frac{\partial p_{1i}^m}{\partial m_q}\right), \tag{9}$$

Here, the sensitivity function is a function of the partial derivatives of the impulse responses which are independent of the source spectrum. Therefore, the full waveform inversion of seismic data does not require the knowledge of the actual source waveform, and this feature is the essence of the proposed inversion scheme.

The actual functional to be minimized consists of the misfit, equation (6), and a model-roughness term to constrain the smoothness on the variation of the model in the updating process. Specifically, it may be written

$$\Phi\left(\mathbf{m}+\delta\mathbf{m}\right) = \phi\left(\mathbf{m}+\delta\mathbf{m}\right) + \lambda\left\|\mathbf{W}_m\delta\mathbf{m}\right\|^2, \tag{10}$$

where $\lambda$ is the Lagrange multiplier that controls relative importance of data misfit and model roughness, and $\mathbf{W}_m$ is an $M \times M$ weighting matrix of the model parameters. When the matrix is diagonal there is no spatial smoothing in the inversion procedure. On the other hand, if the matrix represents a gradient operator its effect is to spatially smooth out the changes. Minimization of functional (10) with respect to the perturbation $\delta\mathbf{m}$ in model parameters results in a system of normal equations

$$\left(\mathbf{J}^T\mathbf{W}_d{}^T\mathbf{W}_d\mathbf{J} + \lambda\mathbf{W}_m{}^T\mathbf{W}_m\right)\delta\mathbf{m} = -\mathbf{J}^T\mathbf{W}_d{}^T\mathbf{W}_d\left(\mathbf{T}^m - \mathbf{T}^d\right), \tag{11}$$

from which the model parameter at the ($k$+1)-th iteration is updated to

$$m_q^{k+1} = m_q^k + \delta m_q^k, \quad q = 1, 2, ..., M \ . \tag{12}$$

The iteration stops when the change in model parameters is below a preset tolerance, typically given in terms of root-mean-square (rms) in misfit.

## NUMERICAL EXAMPLES

The model used for the test is a broken dipping fault in a background of 3000 m/s constant velocity as shown in Figures 1-a and 3-a. The fault consists of a 6 m thick low velocity (2500 m/s) layer overlain by another 6 m thick high velocity (3500 m/s) layer. A crosshole configuration is used for the exercise, with the source borehole at $x$ = - 45 m and the receiver borehole at $x$ = 45 m. A total of 21 line sources are used with an equal vertical separation of 9 m, and the same number and separation are for the receivers. For each source, the pressure wavefields computed at the 21 receiver positions have been normalized by the first pressure wavefield, resulting in 21 normalized wavefields. The number of frequencies used is 10; starting from 10 Hz to 100 Hz, linearly separated by 10 Hz. Prior to inversion, a 5% Gaussian noise was added to the synthetic data. A grid consisting of 200 by 260 elements of uniform cell size, 3 m by 3 m, has been used to compute pressure wavefields using FEM. The domain to be reconstructed was 120 m by 180 m (40 by 60 elements), containing a total of 2400 velocity parameters. It took 250 MB of memory and 18 hours per iteration on a Pentium 4, 1.5 GHz PC. The size of the matrix from equation (11) is modest for the test model, so we solved it using QR decomposition with successive Householder transformations. The Lagrange multiplier $\lambda$ is automatically selected in the inversion process. The selection procedure starts with executing a given number, say *nl*, of inversions using *nl* different multipliers that are separated equally in logarithmic scale. The same Jacobian matrix is used *nl* times, with only different $\lambda$ values, at this step. As a result *nl* updated parameter sets are produced, followed by *nl* forward model calculations resulting in *nl* data misfits. A reasonable choice for the model parameter and the Lagrange multiplier update would be the one that produces the least data misfit.

The proposed inversion scheme was tested using two initial models of different uniform velocities; 3300 m/s and 2850 m/s. For each initial model, we first carried out conventional inversion assuming that the source function is known. The functional to be minimized is the misfit between the pressure wavefield data and the numerically computed ones, which can be obtained by convolving the impulse response obtained from equation (4) and the source waveform. For simplicity, the source waveform used in this study is an impulse source. For the first model with its initial velocity of 3300 m/s, the resulting velocity image is shown in Figure 1-b. We also obtained the velocity structure using the proposed normalized wavefield approach, and the result is shown in Figure 1-c. Here, the functional to be minimized is the misfit in the normalized wavefield, not in the pressure wavefield, and therefore the source function is not involved in the inversion process. In this exercise we used *nl* =3 in each iteration to select parameter update and Lagrange multiplier. After 6 iterations for the normalized wavefield approach and 7 iterations with conventional approach with an impulse source, two results appear almost identical. Note that the normalized wavefield approach has one less data than the conventional approach with known source function because data at one receiver position was used to normalize the others. The fault is imaged correctly, but the images are smeared both vertically and horizontally mainly due to the constraint of imposed model smoothness for stabilizing the inversion. The smearing

appears to be more pronounced, especially in the vertical direction, for the case of normalized wavefield approach. Figure 2 show that the rms misfits for the inversion of normalized wavefield converges faster than the conventional approach. The rms misfit used for the conventional approach is defined as

$$\mathrm{rms}_d = \sqrt{\frac{\delta\mathbf{D}^T\delta\mathbf{D}}{NEQD}} = \sqrt{\frac{1}{NEQD}\sum_{i=1}^{NS}\sum_{j=1}^{NG}\sum_{k=1}^{NFREQ}\left(\frac{\delta d_{ji}^{T}\delta d_{ji}}{|d_{ji}^{d}|^2}\right)_k},$$

where **D** indicates pressure wavefield data, superscript $T$ indicates conjugate transpose, $\delta d_{ji} = (d_{ji}^{d} - d_{ji}^{m})$, and $NEQD = 2 \times NFREQ \times NS \times NG$. The rms misfit used for the normalized wavefield approach is

$$\mathrm{rms}_t = \sqrt{\frac{\delta\mathbf{T}^T\delta\mathbf{T}}{NEQT}} = \sqrt{\frac{1}{NEQT}\sum_{i=1}^{NS}\sum_{j=1}^{NG-1}\sum_{k=1}^{NFREQ}\left(\frac{\delta t_{ji}^{T}\delta t_{ji}}{|t_{ji}^{d}|^2}\right)_k},$$

where **T** indicates normalized wavefield data, $\delta t_{ji} = (t_{ji}^{d} - t_{ji}^{m})$, and $NEQT = 2 \times NFREQ \times NS \times (NG\text{-}1)$. Note that the Lagrange multiplier changes as iteration is continued. The second example starts with an initial guess of a 2850 m/s uniform velocity. For this initial model the inversion converges faster to the same level (Figure 4) as the one with the 3300 m/s initial model. It took 4 iterations for the conventional approach and 3 iterations for the normalized wavefield approach. The fast and stable convergence may have been the result of the better initial model chosen. The inverted velocity distribution for the conventional approach and the normalized wavefield approach are shown in Figures 3-b and 3-c, respectively. The qualities of the inversion with the 2850 m/sec initial model appear to be better than the ones with the 3300 m/s initial model (Figures 1-b and 1-c).

The overall quality of the inversion may improve by adopting a staged approach from low frequencies to high frequencies (e.g., Song et al., 1995; Pratt, 1999a), instead of inverting all frequency information simultaneously. Further improvement may be achieved by using denser deployment of sources and receivers with a sampling rate on the order of cell size.

## CONCLUSIONS

A full waveform inversion scheme based on normalized wavefield has been proposed and the validity of the scheme is successfully demonstrated using a simple 2-D synthetic model. Normalized wavefield for a source depends only on the subsurface model and the position of the source, and is independent of the source spectrum by construction. The highlight of this paper is that full waveform inversion of seismic data can be achieved using the normalized wavefield, and that potential inversion errors due to source estimation involved in conventional full waveform inversion methods can be eliminated. Extension of the proposed scheme to 3-D problems with applications to real data requires further investigation.

## ACKNOWLEDGMENTS

This work was supported by the Office of Basic Energy Sciences, Engineering and Geosciences Division of the U.S. Department of Energy under Contract No. DE-AC03-76SF00098. The first author acknowledges the professional leave granted by the Earth Sciences Division of the E. O. Lawrence Berkeley National Laboratory. The proposed idea was implemented during this period. Korea Science and Engineering Foundation (R01-2001-000071-0) provided support for the second author to participate in this study. Authors would like to thank an Associate Editor and anonymous reviewers for their valuable suggestions and comments in improving the quality of this paper.

## REFERENCES

Bertsekas, D. P., 1982, Enlarging the region of convergence of Newton's method for constrained optimization: J. Optimization Theory Applications, **36**, 221-251.

Cerveny, V., and Soares, J. E. P., 1992, Fresnel volume ray tracing: Geophysics, **57**, 902-915.

Frazer, L. N., Sun, X., and Wilkens, R. H., 1997, Inversion of sonic waveforms with unknown source and receiver functions: Geophys. J. Int., **129**, 579-586.

Frazer, L. N., and Sun, X., 1998, New objective functions for waveform inversion: Geophysics, **63**, 213-222.

Humphreys, E., and Clayton, R. W., 1988, Application of back-projection tomography to seismic traveltime problems: J. Geophys. Res., **93**, 1073-1085.

Kormendi, F., and Dietrich, M., 1991, Nonlinear waveform inversion of plane-wave seismograms in stratified elastic media: Geophysics, **56**, 664-674.

Marfurt, K. J., 1984, Accuracy of finite-difference and finite-element modeling of the scalar and elastic wave equations: Geophysics, **49**, 533-549.

Minkoff, S. E., and Symes, W. W., 1997, Full waveform inversion of marine reflection data in the plane-wave domain: Geophysics, **62**, 540-553.

Nolet, G., 1985, Solving or resolving inadequate and noisy tomographic systems: J. Comp. Phys., **61**, 463-482.

Oldenburg, D. W., McGillivray, P. R., and Ellis, R. G., 1993, Generalized subspace methods for large-scale inverse problems: Geophys. J. Int., **114**, 12-20.

Peterson, J. E., Paulson, B. N. P., and McEvilly, T. V., 1985, Applications of algebraic reconstruction techniques to crosshole seismic data: Geophysics, **50**, 1566-1580.

Plessix, R.- E., and Bork, J., 1998, A full waveform inversion example in VTI media: 68th Ann. Internat. Mtg., Soc. Expl. Geophys., Expanded Abstracts, 1562-1565.

Pratt, R. G., 1990, Inverse theory applied to multi-source cross-hole tomography, Part II: elastic wave-equation method: Geophys. Prosp., **38**, 311-330.

____, 1999a, Seismic waveform inversion in frequency domain, Part 1: Theory and verification in physical scale model: Geophysics, **64**, 888-901.

——, 1999b, Seismic waveform inversion in frequency domain, Part 2: Fault delineation in sediments using crosshole data: Geophysics, **64**, 902-914.

Scales, J. A., Gersztenkorn, A., and Treitel, S., 1988, Fast solution of large sparce, linear systems: Application to seismic traveltime tomography: J. Comp. Phys., **75**, 314-333.

Sen, M. K., and Stoffa, P. L., 1991, Nonlonear one-dimensional seismic waveform inversion using simulated annealing: Geophysics, **56**, 1624-1638.

Sheng, J., and Schuster, G. T., 2000, Finite-frequency resolution limits of traveltime tomography for smoothly varying velocity models: 70th Ann. Internat. Mtg., Soc. Expl. Geophys., Expanded Abstracts, 2134-2137.

Tarantola, A., 1987, Inverse Problem Theory: Methods for Data Fitting and Parameter Estimation: Elsevier, Amsterdam.

Vasco, D. W., 1991, Bounding seismic velocities using a tomographic method: Geophysics, **56**, 472-482.

Vasco, D. W., Peterson, Jr., J. E., and Majer, E. L., 1995, Beyond ray tomography: Wavepaths and Fresnel volumes: Geophysics, **60**, 1790-1804.

Zhou, C., Schuster, G. T., Hassanzadeh, S., and Harris, J. M, 1997, Elastic wave equation traveltime and wavefield inversion of crosswell data: Geophysics, **62**, 853-868.

Zienkiewicz, O. C., and Taylor, R. L., 1989, The Finite Element Method, 4th ed.: McGraw-Hill, London.

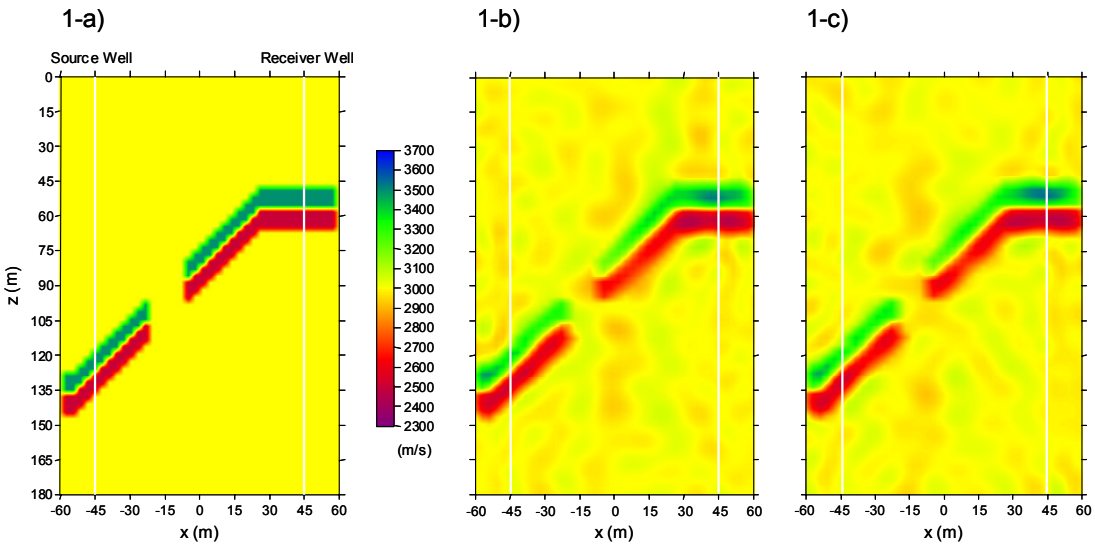


Fig. 1. Comparison of full waveform inversion results using a fault model in a background of 3000 m/s constant velocity. Starting model used for the inversion is a 3300 m/sec uniform velocity. a) A 2-D velocity model. b) Inversion result using pressure wavefield with impulse source. c) Inversion result using normalized wavefield.

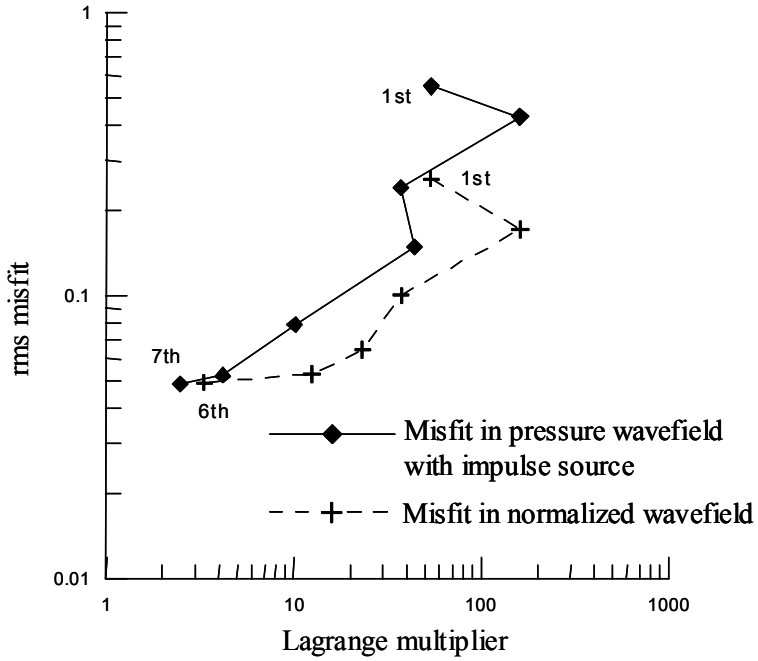


Fig. 2. Comparisons in convergence in rms misfits and associated Lagrange multiplier as a function of iteration during the full waveform inversion with a 3300 m/sec uniform velocity starting model. Pressure wavefield was generated using an impulse source.

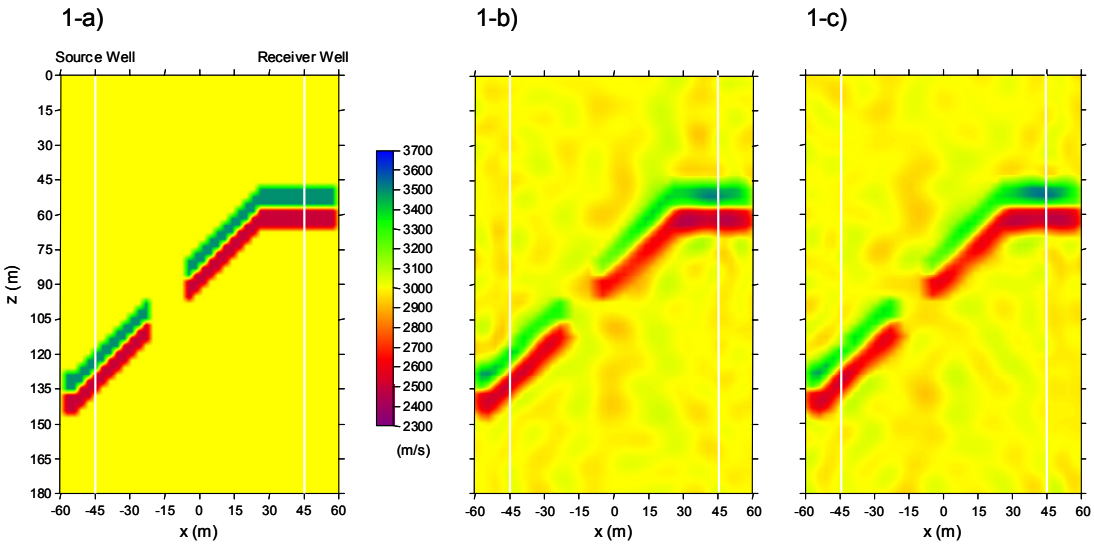


Fig. 3. Comparison of full waveform inversion results using a fault model in a background of 3000 m/s constant velocity. Starting model used for the inversion is a 2850 m/sec uniform velocity. a) A 2-D velocity model. b) Inversion result using pressure wavefield with impulse source. c) Inversion result using normalized wavefield.

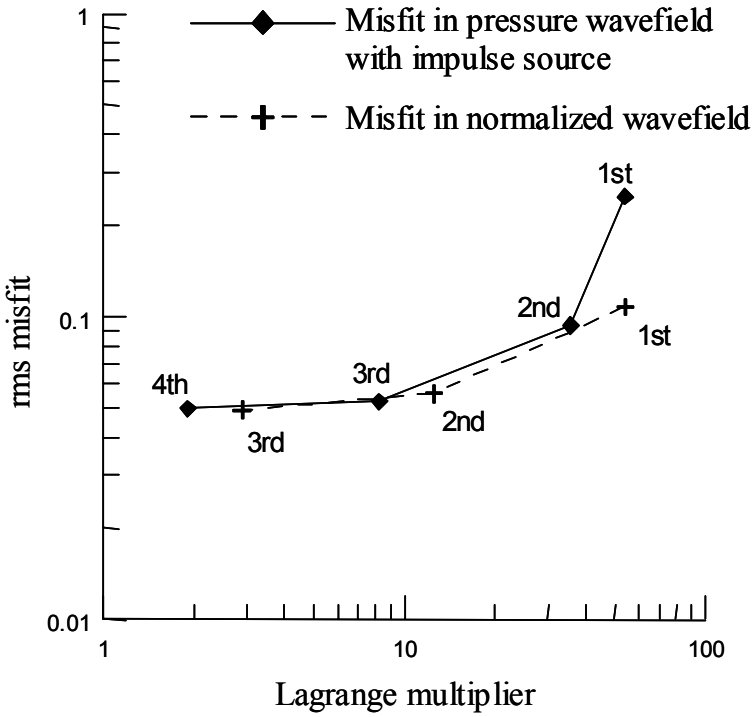


Fig. 4. Comparisons in convergence in rms misfits and associated Lagrange multiplier as a function of iteration during the full waveform inversion with a 2850 m/sec uniform velocity starting model. Pressure wavefield was generated using an impulse source.